Geiger Counter

James Amarel and Gabriel Oman

March 17, 2017

1 Goal

Our aim in this lab is to investigate radioactive properties of a ^{226}Ra sample and determine the background radiation level of our environment. We first characterize our Geiger-Mueller counter and determine its operating parameters. Then we measure the number of detected decays in a certain time window and make necessary corrections of these measurements to determine source radioactivity rates. The results the high count rate process of Radium decay are compared with the Gaussian distribution, and the low count rate data of background decay is compared with the Poisson distribution.

2 Introduction/Background

When describing elementary particles it is necessary to adopt a view of anything that can happen will happen. So long as the process does not violate any conservation symmetries, particles may undergo a variety of transformations, although the probability is decreased as the transformations become more complex [2]. Given the opportunity, nuclei will eventually transform to a lower energy level and emit decay products. Beta decay and gamma decay, two of the three common decay processes, rely on the exchange of gauge bosons to mediate a weak or electromagnetic interaction. The third common decay process is alpha decay, which requires the nuclear force and a nonzero probability for quantum tunneling [1]. One can imagine the alpha particle as a separate entity caught in the potential well of the residual strong force until enough time has elapsed to dig through the barrier. Once escaped, alpha particles are immediately accelerated by the Coulomb force of the positively

charged nucleus. As Harris explains, the He nucleus has an abnormally large binding energy per nucleon ratio. And, the binding energy per nucleon for heavier nuclei decreases monotonically as the nucleon number increases [3]. So a large and bulky atom will prefer to discard a tightly bound Helium nucleus if the decay increases the binding energy per nucleon of the parent nucleus. The reduction in energy is transferred to the daughter nucleus as kinetic energy, which propels the alpha emission with enough energy to ionize atoms along its trajectory.

A Geiger-Mueller counter (GM tube) can count each radiated alpha particle by collecting electrons liberated from a mica screen by the alpha radiation. Electrons are drawn to an electrode in a cylindrical cavity and each current pulse generated by adsorption is recorded. But, for a short time window after each Geiger pulse, a conducting plasma forms around the electrodes which arranges in effort to cancel the electric field. As consequence, no pulses are recorded during this dead time. A solution for this affect is to estimate the true number of counts by introducing a correction factor

$$N_{true} = \frac{N_{obs}}{1 - R_{obs}\tau} = CN_{obs} \tag{1}$$

where C scales the measured counts to the true counts according to the expected emission rate, R_{obs}, and the dead time, τ, which is characteristic to each GM unit. A counting circuit built in to the GM tube is capable of filtering any noise pulses that do not exceed a threshold voltage. Additionally, the properties of a GM tube give it three different operating regions depending on the tube voltage. It is desirable to work in the beginning of the third, high voltage, region which is called the Geiger region. In the Geiger region, an ion plasma is sustained along the high-field anode, which causes all pulse heights to be nearly equivalent and blurred together within a time window, which effectively combats the possibility of over counting when a single decay product causes multiple ionizations. Also, the conducting plasma can reorient according to the Electric field in the tube, which causes the number of counts to be only weakly dependent upon the tube voltage.

3 Procedures and Data

We used a Geiger-Mueller counter to investigate the alpha decay of a ^{226}Ra sample. Our radioactive sample was placed beneath a GM tube, as seen in the

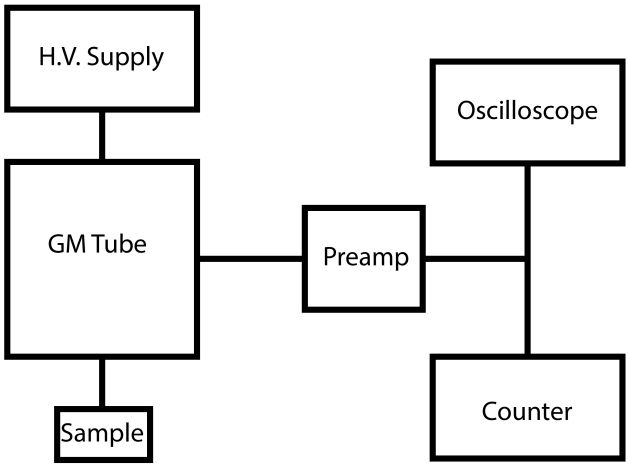

Figure 1: Block diagram outlining the role of each experimental device.

block diagram of Figure 1, which is power by a high voltage supply. Output from the GM tube is amplified and sent to an oscilloscope for display and a counter to determine the decay rate. First, we determined the characteristic dead time of our GM tube by finding the discriminator level of the comparator circuit and the electrode operating voltage. We determine the discriminator level by slowly increasing the electrode voltage from zero and pausing at the point of first counts. Then we measure the height of the barely counted pulses from an oscilloscope and determine the discriminator level to be 920 $\pm$ 20 mV. Next, we find the ideal operating voltage to ensure our GM tube is in the Geiger region by measuring and recording the number of decay counts as a function of the tube voltage. We identified the Geiger region as beginning at 625 volts from Figure 2. To ensure we are within the Geiger region, but still at a reasonable voltage, we chose an operating point of 720 V and remained at this voltage for the rest of our measurements.

Then we measured the pulse width, Δt, of a single pulse from the oscilloscope display, shown in Figure 3, where the upper horizontal line represents the saturated pulse height of 3.02 V and the lower horizontal line marks the discriminator voltage. From Figure 3 we measure a pulse width of $\Delta t = 70$ μs, which is the duration required for a pulse to decay to 37% of its peak height. From Figure 3 we also determined the dead time, $\tau = 478$ μs, by recording the time at which the build up envelope surpasses the discriminator level. And we can determine the full recovery time, $\tau_r = 562$ μs, as the

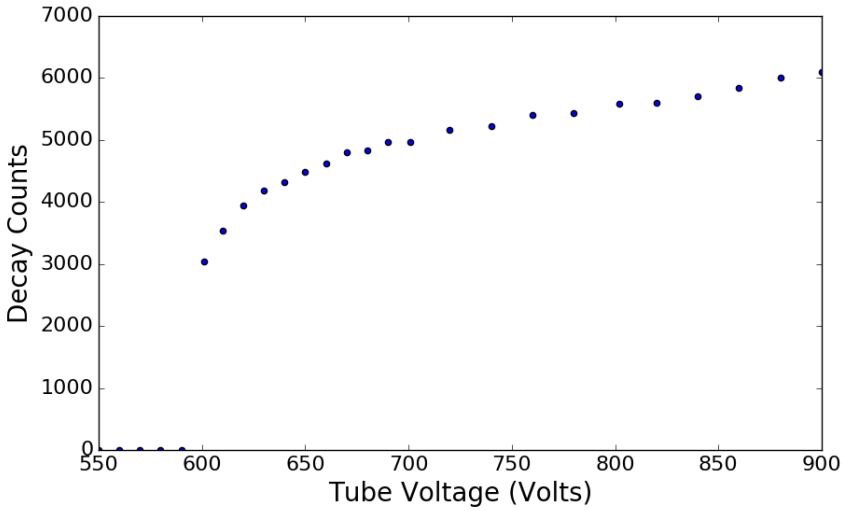

Figure 2: Number of registered counts from a ^{226}Ra source as a function of the Geiger tube voltage.

time required for the build up envelope to reach its full height.

Next, we adjusted the source of our sample such that the count rate was approximately 100 per second and recorded the number of counts in thirty 10 s intervals. A histogram of this data and Gaussian comparison, estimated from the mean of standard deviation all counts, is seen in Figure 4.

At this point we removed the Radium sample so that the GM tube could count the background radiation, which is assumed to be mostly cosmic rays. We recorded thirty decay counts in 100 s, which gives a measured background radiation rate of 0.33 ± 0.05 counts per second. Lastly, we used the radiation rate to estimate that waiting for a time interval of 6.7 seconds would likely result in 2 counts, and then took measurements of the counts during fifty 6.7 s intervals. A histogram of the background radiation counts is seen in Figure 5, which nicely resembles a Poisson distribution.

4 Analysis and Discussion

Figure 2 allows us to determine the range of voltages that make up each performance region of the GM tube. The low voltage behavior of region one

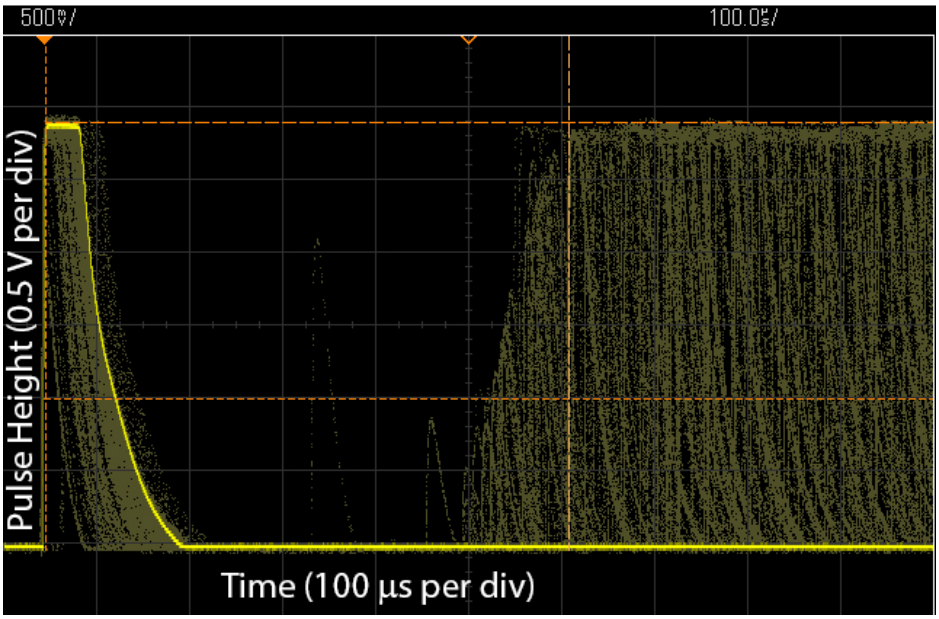

Figure 3: A still image of the oscilloscope trace following a registered pulse. The initial pulse is at time zero, then a dead region follows, and finally an envelope builds to the initial pulse height.

continues until about 590 V, where we begin to see the proportional counting associated with region two. Region two persists until about 620 V, at which the Geiger region begins as outlined previously. By fitting a line to the data of region three, we determine the slope and y-intercept, which allows the following equation to be used to approximate the percent increase in counts

$$\frac{\Delta y}{y} = \frac{m\Delta x}{mx + b} \tag{2}$$

where the slope y is the number of counts, x is the tube voltage, and where $b = 283$ and $m = 6.5$ $[V^{-1}]$. This calculation estimates a 14% increase in counts per 100 V increase in the tube voltage. The largest count rate found in Figure 2 is nearly 6000 per 10 s, then by assuming that the detector records only 10% of the total decays, we estimate the source activity as 0.16 μCi. From Equation 1 and our measured value of $\tau = 478$ μs we correct for the dead time, which is already factored in to the previous histograms. The correction factor is incredibly important in gathering accurate measurements, this is evidenced by the fact that a 1% correction is necessary even the at

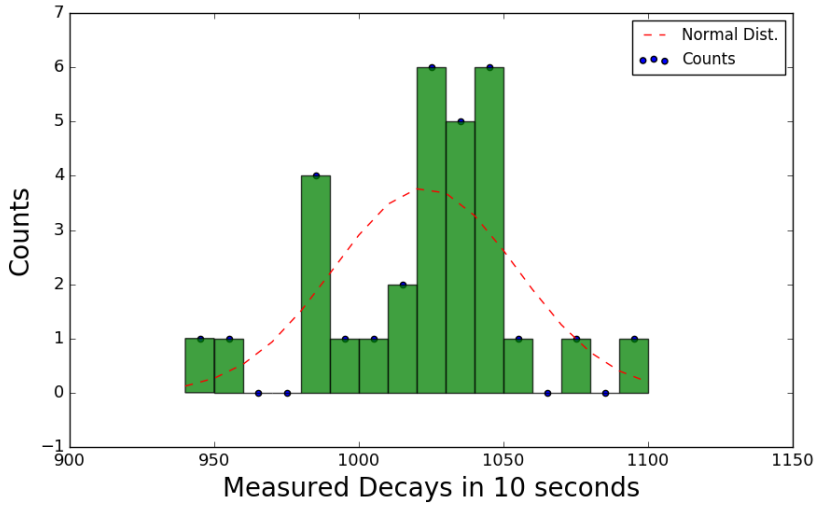

Figure 4: Histogram of the corrected number of decays for 30 ten-second measurements and a Gaussian fit comparison.

low rate of 20 counts per second.

The high count rate data of Figure 4 has the mean decay count $\bar{N} = 1020$, with $\sigma_{th} = \sqrt{\bar{N}} = 32$ and $\sigma_{exp} = 32$, where σ_{exp} is derived from the standard deviation of all measured counts. Prior to rounding, the reliability factor, $\sigma_{exp}/\sigma_{th} = 0.99$, which indicates a Gaussian distribution with good confidence. This is an interesting result because a glance at Figure 4 is not entirely convincing of a Gaussian distribution due to the irregularity in the left side of the peak. Further support our results obeying the Gaussian distribution is found by considering that 22 of the 30 measurements, 73%, lie within $\bar{N} \pm \sigma_{exp}$ and 90% lie within $\bar{N} \pm 2\sigma_{exp}$. $\bar{N}$ is the average number of counts in a ten second interval and so the best value for the average counting rate is determined by $R_{best} = 102 \pm 3$, where the uncertainty in rate is determined from the standard deviation as that is what is required for Poisson processes. Additionally, reducing the uncertainty to the standard deviation of the mean would not reflect the spread in our data.

Our results from the low count rate measurements can be quantitatively shown to agree with the Poisson distribution by comparing number of total counts, N_ν, and the experimental uncertainty, $\sqrt{N_\nu}$, for each bin of Figure 5 with the value predicted by Poisson statistics. Of the five bins in Figure 5,

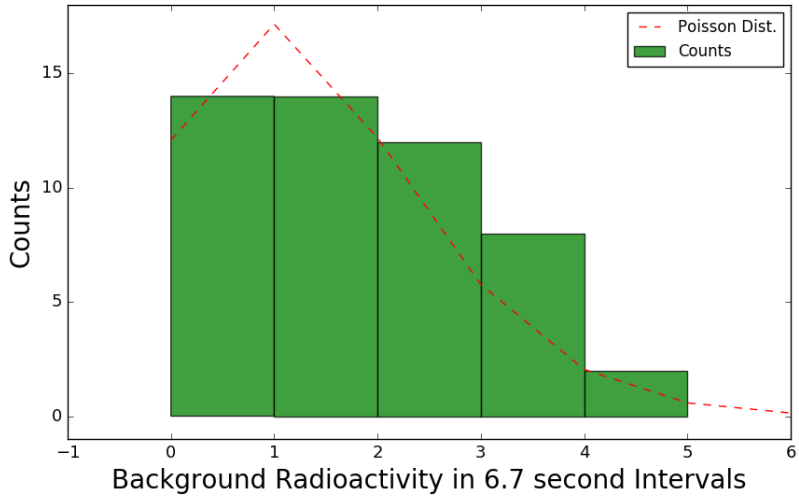

Figure 5: Histogram of the background count data and a comparison with the Poisson distribution.

four of them lie within one standard deviation of the dotted Poisson curve, and all counts lie within two standard deviations of the Poisson predictions.

5 Conclusion

We determined the dead time of our Geiger-Mueller counter by recording the time required for the buildup envelope to surpass the discriminator level. Once the dead time was known, we then corrected for the plasma formation inside our GM tube and then took radioactive decay measurements of both Radium and background radiation to show that that these decay processes can be predicted by a Gaussian or Poisson distribution depending on the count rate. Our measurements of the high count rate process of Radium's alpha decay, seen in Figure 4, were distributed in a reasonably Gaussian manner, with 73% of counts laying within $\bar{N} \pm \sigma_{exp}$ and 90% within $\bar{N} \pm 2\sigma_{exp}$. After the Radium source was removed, we measured the count rate of background radiation, Figure 5, and found great agreement with the Poisson distribution.

References

[1] Jean Belle. Alpha Decay, 2014. URL `https://readingfeynman.org/tag/alpha-decay/`.

[2] David Griffiths. *Introduction to Elementary Particles*. Wiley, 2004.

[3] Randy Harris. *Modern Physics*. Pearson, 1998.